



PCCP

**Time-Resolved Dynamics of Stable Open- and Closed-Shell
Neutral Radical and Oxidized Tripyrrindione Complexes**

Journal:	<i>Physical Chemistry Chemical Physics</i>
Manuscript ID	CP-ART-02-2022-000632.R1
Article Type:	Paper
Date Submitted by the Author:	09-Jun-2022
Complete List of Authors:	Cho, Byungmoon; The University of Arizona, Chemistry and Biochemistry Swain, Alicia; The University of Arizona, Chemistry and Biochemistry Gautam, Ritika; The University of Arizona, Chemistry and Biochemistry; Indian Institute of Technology Kanpur Tomat, Elisa; The University of Arizona, Chemistry & Biochemistry Huxter, Vanessa; The University of Arizona, Chemistry and Biochemistry; The University of Arizona, Physics

SCHOLARONE™
Manuscripts

ARTICLE

Time-Resolved Dynamics of Stable Open- and Closed-Shell Neutral Radical and Oxidized Tripyrrindione Complexes[†]

Byungmoon Cho,^a Alicia Swain,^a Ritika Gautam,^{a,b} Elisa Tomat,^a and Vanessa M. Huxter^{*a,c}Received 00th January 20xx,
Accepted 00th January 20xx

DOI: 10.1039/x0xx00000x

Stable open- and closed-shell Pd(II) and Cu(II) complexes of hexaethyl tripyrrin-1,14-dione (TD1) produce triplet, doublet or singlet states depending on the metal center and the redox state of the ligand. Pd(II) and Cu(II) form neutral TD1 complexes featuring ligand-based radicals, thus resulting in doublet and triplet states, respectively. The reversible one-electron oxidation of the complexes removes an unpaired electron from the ligand, generating singlet and doublet states. The optical properties and time-resolved dynamics of these systems are studied here using steady-state and ultrafast transient absorption (pump-probe) measurements. Fast relaxation with recovery of the ground state in 10s of picoseconds is observed for the copper neutral radical and oxidized complexes as well as for the palladium neutral radical complex. Significantly longer timescales are observed for the oxidized palladium complex. The ability to tune the overall spin state of the complexes through their stable open shell configurations as well as the reversible redox activity of the tripyrrolic systems makes them particularly interesting for catalytic applications as well as exploring magnetism and conductivity properties.

Introduction

In photosynthetic systems, tetrapyrrolic compounds form a primary class of light harvesting pigments,¹ from linear bilins in cryptophyte antennas^{2, 3} to the macrocyclic chlorin- or bacteriochlorin-based chlorophyll⁴ and bacteriochlorophyll.⁵ Numerous linear or macrocyclic oligopyrroles, including tetrapyrrolic porphyrins in heme, are found in nature in a variety of roles. Many oligopyrrolic molecules have the capacity to bind metals, often producing redox-active complexes. The ability of these systems to accept or donate electrons plays a central role in biological processes as diverse as water splitting in photosynthesis to enzymatic catalysis and metabolism.

While tetrapyrrolic molecules are common in biological systems, tripyrroles are comparatively rare. Examples of naturally occurring tripyrroles include prodiginines^{6, 7} and some heme metabolites such as uroerythrin.^{8, 9} Although tripyrroles are rather uncommon in nature, they are effective tridentate ligands for metal coordination.^{10, 11}

In the current paper, we present the ultrafast dynamics of the tripyrrolic ligand hexaethyl tripyrrin-1,14-dione (TD1),¹²⁻¹⁴ bound to either a copper(II) or palladium(II) center.¹⁵⁻¹⁷ Tripyrrindiones have the structural scaffold of metabolite uroerythrin and they are related to the family of tripyrrins and other linear tripyrroles.^{18, 19} In addition, recent studies have shown that tripyrrindiones are capable of hosting delocalized

unpaired electrons and undergo reversible ligand-based redox chemistry in metal complexes that are stable at room temperature.^{16, 17} Due to their ability to accommodate unpaired spins on both the metal and the ligand, the tripyrrindione complexes can adopt stable closed- and open-shell configurations with singlet, doublet, or triplet ground and excited states depending on the nature of the metal center and the overall redox state of the complex.

The TD1 ligand binds in a meridional tridentate fashion through the three pyrrolic nitrogen donors, as shown in Figure 1, forming planar complexes with Pd(II), Ni(II) and Cu(II) ions.² A water molecule is bound to the fourth coordination site in the square planar structure. This aqua ligand is hydrogen-bound to the carbonyl groups of the tripyrrolic ligand and cannot be easily replaced by chemical or electrochemical methods. Spectroscopic and electrochemical data have shown that the tripyrrindione ligand in these neutral complexes binds as a dianionic radical featuring an unpaired electronic spin that is delocalized throughout the π system of the ligand.^{16, 17} Complexes of tripyrrindione in other redox states (i.e., coordinating as a monoanionic or trianionic diamagnetic system) have also been reported.^{15, 16} Tripyrrindiones, therefore, act as redox-active ligands and can expand the number of available electrons for redox processes beyond the metal center.¹¹ In addition, complexation with transition metal ions offers possibilities to form complex structures including coordination polymers and π -stacked dimers.^{15, 20, 21}

In this paper, we present steady-state and femtosecond time-resolved pump-visible continuum probe measurements of TD1 complexes of copper and palladium in both the neutral radical and oxidized forms. One-electron oxidation of the neutral radical copper and palladium complexes removes an electron from the ligand, leaving the oxidation state of the

^a Department of Chemistry and Biochemistry, The University of Arizona, Tucson, Arizona, 85721.

^b Current address: Department of Chemistry, Indian Institute of Technology Kanpur, Kanpur 208016, India

^c Department of Physics, The University of Arizona, Tucson, Arizona, 85721.

[†] Electronic Supplementary Information (ESI) available: See DOI: 10.1039/x0xx00000x

central metal unchanged. The series of complexes studied here, comprising neutral radical and oxidized forms with Cu(II) d^9 and Pd(II) d^8 metal centers, allow us to compare two square planar complexes with paramagnetic and diamagnetic metal centers to observe the effects of changing overall spin quantum number and exchange coupling on the ultrafast electronic dynamics. While the ligand field strength is expected to be different in the copper and palladium complexes based on 3d and 4d orbital interactions respectively, the main electronic transitions are ligand-dominated and are similar in terms of both energy and lineshape. The tripyrrolic ligands can participate in both one-electron oxidation and reduction independent of the metal center, demonstrating their ability to act as redox-active non-innocent ligands and to host stable ligand-based radicals. Here we abbreviate the neutral radical d^9 tripyrrindione–Cu(II) complex $[\text{Cu}(\text{TD1}^*)(\text{H}_2\text{O})]$ and the d^8 tripyrrindione–Pd(II) complex $[\text{Pd}(\text{TD1}^*)(\text{H}_2\text{O})]$ as TD1–Cu and TD1–Pd, respectively.

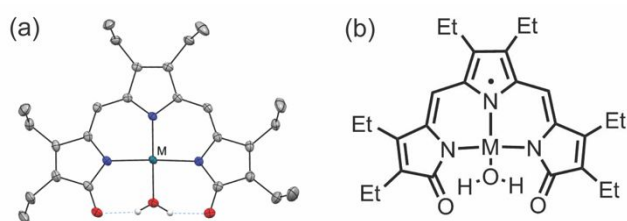


Figure 1: Structure of the TD1-metal complexes with coordinated water molecule. In both panels, the M label represents Pd(II) or Cu(II). The crystal structure of $[\text{Pd}(\text{TD1}^*)(\text{H}_2\text{O})]$ is shown in panel (a). Carbon-bound hydrogen atoms in calculated positions are omitted for clarity (CCDC 1400990). Panel (b) shows the molecular structure of the neutral radical TD1-metal complexes. The unpaired spin density is delocalized over the entire ligand system.

The oxidized, cationic complexes $[\text{Pd}(\text{TD1}_{\text{ox}})(\text{H}_2\text{O})]^+$ and $[\text{Cu}(\text{TD1}_{\text{ox}})(\text{H}_2\text{O})]^+$, both of which have a $[\text{BF}_4^-]$ counter ion, are abbreviated as TD1–Cu–Ox and TD1–Pd–Ox.

Using steady-state linear absorption and broadband-probe transient absorption measurements, the optical properties and ultrafast dynamics of the electronic relaxation pathways were measured as a function of solvent dependence and oxidation state. We present a series of transient absorption measurements of the neutral radical and oxidized complexes in acetonitrile (MeCN), *N,N*-dimethylformamide (DMF) and toluene. The ultrafast dynamics were mapped using global analysis²² of the transient absorption measurements.

Experimental

The redox-active TD1-Pd and TD1-Cu as well as one-electron oxidized TD1–Cu–Ox and TD1–Pd–Ox complexes were synthesized according to previously reported methods.^{16, 17} The metal complexes were dissolved in dry/distilled toluene, MeCN, and DMF in preparation for the steady-state and ultrafast measurements. The steady-state absorbance and fluorescence measurements were performed using 2 mm pathlength cuvette in a Cary 100 and a Cary Eclipse, respectively. The experimental apparatus used to collect femtosecond pump-probe transient spectra has been previously described.²³ Briefly, 100 fs, 1KHz, 800 nm pulses were generated by a Spectra-Physics Solstice

Ti:Sapphire regenerative amplifier. The output of the Ti:Sapphire regenerative amplifier was used to pumping a Light Conversion TOPAS to produce spectrally tunable visible pulses and also to generate a white-light continuum probe using a sapphire plate. The output from the TOPAS was used for the tunable excitation or pump pulses and the white-light continuum was used for the probe. All measurements were made at room temperature. Additional experimental details can be found in the Electronic Supplementary Information (ESI).

Results and Discussion

Beginning with steady-state measurements, Figure 2 shows the absorption spectra of (a) TD1–Cu, and (b) TD1–Pd complexes as well as the oxidized (c) TD1–Cu–Ox and (d) TD1–Pd–Ox complexes dissolved in toluene, DMF, and MeCN. The absorption spectra of the neutral radical metal complexes in Fig. 2 (a) and (b) show the main absorption band in the visible at ~ 600 nm. There are also transitions with low oscillator strength in the near-IR at ~ 730 nm, ~ 835 nm and ~ 900 nm (the ~ 835 nm and ~ 900 nm peaks are not shown), which are characteristic of ligand-based radicals of oligopyrrolic complexes. Ligand-only absorption spectra in the same solvents shows the main band in the visible at ~ 480 nm.²³ Previous work on linear oligopyrroles,^{8, 24} a recent DFT calculation on a related linear tripyrrin,²⁵ as well as electrochemical measurements on the TD1-Pd complex¹⁶ indicate that the two main bands originate from π – π^* transitions. Both bands red-shift upon binding metal cations. This red-shift is consistent with ionochromic effects often observed in many metal-chelating conjugated polymers containing pyridyl moieties.^{26–28} The red-shift is thought to occur when metal ion coordination to a polymer leads to conjugation enhancement through rigidification and electron density variation in the polymer backbone. Metal ion coordination to three pyrrolic nitrogens in the tripyrrindione backbone is likely to cause similar effects as the lower energy band is narrower in

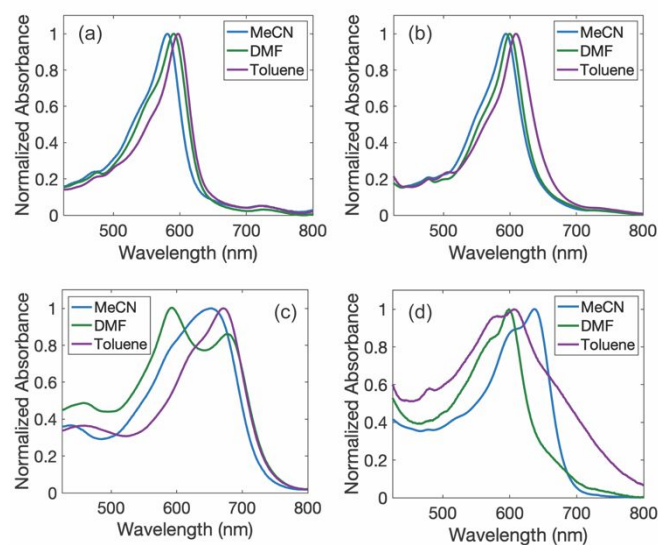


Figure 2: Normalized steady-state absorption spectra of neutral radical (a) TD1–Cu and (b) TD1–Pd complexes as well as the oxidized complexes (c) TD1–Cu–Ox and (d) TD1–Pd–Ox dissolved in toluene (purple), DMF (green), and MeCN (blue).

the metal complex than in the free ligand, consistent with increased rigidity.

As shown in Figure 2 (a) and (b), the absorption spectra of the neutral radical complexes are only weakly solvent dependent. We did not observe polarity-dependent spectral shifts associated with charge-transfer states or changes in spectral features caused by axial coordination of solvent molecules. Coordinating solvents such as MeCN do not alter the primary coordination sphere of tripyrrindione complexes, in which the ligand maintains a planar tridentate coordination mode. The largest shift observed for the transition at ~ 600 nm was 415 cm^{-1} for TD1-Pd, and 462 cm^{-1} for TD1-Cu (in toluene and MeCN). In comparison, the free ligand has a larger solvatochromatic shift, where the difference between the peak maxima in the same two solvents is 854 cm^{-1} , nearly double that of the TD1-Pd and TD1-Cu complexes.²³

The weak solvent effects displayed by the neutral radical metal ion complexes contrast with those observed for the oxidized form of the TD1-metal ion complexes, TD1-Cu-Ox and TD1-Pd-Ox, shown in Fig. 2 (c) and (d). The absorption spectra of the oxidized complexes have larger variations in band peak positions and broader lineshapes. The one-electron oxidation of both the copper and the palladium complexes removes an electron from the tripyrrindione creating a monoanionic tridentate ligand while maintaining the oxidation state of the metal.¹⁶ Both the peak position and lineshape of the absorption spectra of the oxidized copper complexes are dependent on the solvent environment, although neither the peak positions for TD1-Cu-Ox or TD1-Pd-Ox follow a general trend relative to the static dielectric constants of the solvents [toluene (2.38), MeCN (35.94), DMF (36.71)]. In DMF, the absorption spectrum of the oxidized complexes evolved as the samples aged in solution. This was likely due to the oxidized complex slowly reverting to the neutral radical form. Both the maximum and the

approximate lineshape of the higher energy peak in the absorption spectrum for the TD1-Cu-Ox complex in DMF is consistent with the absorption of the neutral radical TD1-Cu as shown in Fig. 2(a).

Steady-state excitation-emission scans for both metal complexes in all four solvents across the UV-Vis range showed no discernible photoluminescence. Fluorescence quenching in metal-bound porphyrins is well known when the metal centers are paramagnetic open-shell, such as Cu^{2+} (d^9), or heavy metal diamagnetic closed-shell, such as Pd^{2+} (d^8).^{29, 30} This can be due to the presence of a low-lying metal-centered excited state or a triplet state. DFT calculations of open- and closed-shell metal porphyrins identified a manifold of states below the $\pi-\pi^*$ lowest energy excited state³¹ which are thought to facilitate rapid relaxation.³²⁻³⁴ In non-fluorescent Cu(II) porphyrin,³⁵ ligand-to-metal charge-transfer states greatly enable intersystem crossing into $\pi-\pi^*$ triplet states and the subsequent recovery of the ground state.³⁴⁻³⁹ The lack of fluorescence in Pd(II) porphyrins is discussed in early experimental studies.^{29, 39-42} It is likely that the metal ions similarly influence the fluorescence quenching in the TD1-metal complexes. Lowered symmetry DFT calculations on the related tripyrrin show two bands: one Soret-like at ~ 350 nm and one Q-like at ~ 530 nm, for the $\pi-\pi^*$ states situating them at higher energies than typical Soret- and Q-band in porphyrins.²⁵ This makes metal-assisted deactivation plausible since the metal d-orbital energies are likely similar when bound to TD1 or to porphyrin.⁴³ The role of the metal center in mediating relaxation is further supported by steady-state photoluminescence measurements on the d^{10} Zn(II) complex, which is highly fluorescent in polar solvents.⁴⁴

Ultrafast relaxation dynamics were observed using broadband-probe transient absorption measurements. Representative data for the oxidized and neutral radical forms

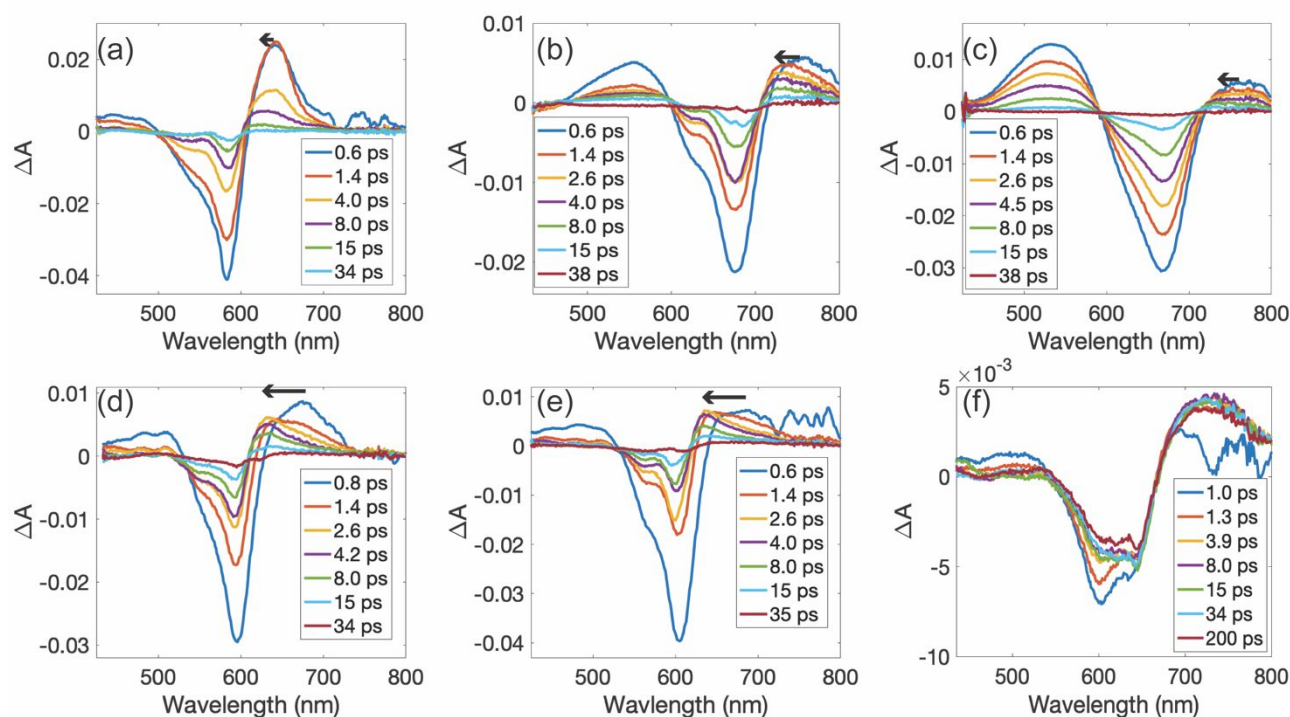


Figure 3: Transient absorption spectra of neutral radical and one-electron oxidized forms of the copper and palladium tripyrrindione complexes. The top row, panels (a), (b) and (c), presents data for copper complexes while the bottom row, panels (d), (e) and (f), presents data for palladium complexes. Panel (a) shows the transient absorption data for the neutral radical TD1-Cu complex in MeCN, (b) for the oxidized TD1-Cu-Ox complex in toluene, and (c) for the oxidized TD1-Cu-Ox complex in MeCN. Panel (d) shows the transient absorption data for the neutral radical TD1-Pd complex in MeCN, (e) for the neutral radical TD1-Pd complex in DMF, and (f) for the oxidized TD1-Pd-Ox complex in MeCN. The arrows indicate blue shifts. All data presented here was collected at room temperature.

of the copper and palladium complexes is shown in Figure 3. The top row, panels (a), (b), and (c), presents the transient absorption spectra at selected time slices for copper complexes while the bottom row, panels (d), (e), and (f), presents the data for palladium complexes. Transient absorption data collected for additional solvent environments is presented in the ESI, Figures S1 and S2. The transient absorption measurements were performed exciting the lowest energy ligand π - π^* transition that has significant oscillator strength. For the neutral radical complexes, laser pulses centered at 600 nm were used for excitation, while excitation pulses centered at 640 nm were used for TD1-Cu-Ox and TD1-Pd-Ox in MeCN, and 675 nm for TD1-Cu-Ox in toluene and TD1-Cu-Ox in DMF.

All the TA data is characterized by a ground state bleach (GSB) at the energy of the main π - π^* transition as well as excited state absorption (ESA) contributions both at the high and low energy sides of the bleach. A feature associated with stimulated emission (SE) is not directly observed in the data although it may be hidden under the positive region to the low energy side of the ground state bleach, where there is a significant ESA contribution in all traces. The lack of SE contributions is consistent with the fact that we did not observe fluorescence for the complexes studied here.

As shown in Figure 3 (d) and (e), the transient absorption data obtained for the palladium neutral radical complex is relatively insensitive to solvent. The same insensitivity is observed for the copper neutral radical complex. The minimal effect of the solvent is also seen in the steady-state absorption data shown in Figure 2 (a) and (b). We observe the same solvent insensitivity in transient absorption data for both the palladium and copper oxidized complexes. Representative data for the oxidized copper complex is shown in Figure 3 (b) and (c) and for the oxidized Pd complex in panel (f). This is surprising given the spectral shifts observed for the oxidized complexes in the steady-state absorption (Figure 2 (c) and (d)). In addition to polarity and basicity, the solvents used here differ in viscosity, ranging from 0.347 mPa·s for MeCN to 0.94 mPa·s for DMF at 298 K. However, no significant effect due to varying viscosity, polarity or basicity was observed in the transient absorption data. These patterns indicate that the relaxation dynamics depend primarily on the identities of the metal centers and the overall oxidation state of the complex.

Representative transient absorption data for the copper neutral radical complex is shown in Figure 3 (a). It is characterized by a GSB around 585 nm (the negative-going peaks coincide with the peak of the main π - π^* transition), an ESA on either side of the bleach, one peaked \sim 645 nm, and another having a flatter feature with smaller amplitude extending to the blue. The ESA features appear within our instrument response. The ESA and the GSB decay simultaneously in 10s of picoseconds. The transient absorption data was fit using global analysis²² to identify common kinetic components. Kinetic traces with fits and evolution associated decay spectra from the global analysis can be found in the ESI.

For TD1-Cu, two timescales were identified ranging from 1.7 to 2.4 ps, and from 7.8 to 13.2 ps. The timescales are listed in Table 1. Both ESA features rise within pulse overlap. The higher energy ESA decays rapidly, followed by the near simultaneous decay of the GSB and the lower energy ESA. This occurs across all samples regardless of solvent. We observed a small amount of residual scatter from the pump excitation in all measurements. The ESA centered at 645 nm appears within the instrument response and undergoes a blueshift of approximately 15 nm, as indicated by an arrow in the figure. No blueshift is observed in the GSB.

Figure 3 (b) and (c) present transient absorption data for the oxidized copper complexes in toluene and MeCN respectively. The data is characterized by a GSB at the energy of the main π - π^* transition as well as ESA contributions to both the high and low energy sides of the GSB feature. The ESA and the GSB decay simultaneously. A global analysis of the data across the three solvents here returned the following timescales: 1.5 to 2.3 ps and 10.7 to 11.5 ps. The timescales obtained from the global analysis are presented in Table 1. We observe a rapid blue shift in the ESA to the low energy side of the GSB centered at 740 nm of approximately 20 nm in all solvents that occurs in approximately 2 ps. No blueshift was observed in the GSB. Both ESA features and the GSB decay nearly simultaneously with little variation across solvents.

Transient absorption of the neutral radical TD1-Pd complex in MeCN and DMF is shown in Figure 3 (d) and (e), respectfully. From this data, two timescales were found in all three solvents, ranging 0.5–0.8 ps, and 7.4–11.4 ps. The timescales obtained from the global analysis are presented in Table 1. The initial spectrum following the instrument response shows a bleach around 600 nm and excited state absorption features on either side of the bleach, initially centered around at 475 nm and 690 nm. The 475 nm excited state absorption feature rapidly decays to zero while at the same time the 690 nm ESA undergoes a significant blue-shift of approximately 60 nm. No blue-shift was observed for the GSB. The remaining absorption and bleach features simultaneously decay of within tens of ps to zero (the near zero non-decaying amplitude is associated with 600 nm pump scatter).

Figure 3(f) presents transient absorption data for the oxidized TD1-Pd-Ox complex in MeCN. Unlike the transient absorption data for the other molecules, the oxidized palladium complex has a long-lived excited state and undergoes little spectral evolution. The data shows a GSB centered at 620 nm, with two ESA contributions centered at 500 nm and 740 nm. Global analysis identified three timescales in the three solvents, 0.4–1.0 ps, 8–60 ps, and 3–6 ns, which are presented in Table 1. This last timescale is not well characterized by our experiment as it is longer than the maximum time delay. The ESA at 740 nm rises within the first 1.5 ps while the other ESA at 500 nm decays rapidly. The GSB decreases to about 1/3 of its initial value within tens of ps. The remaining GSB and the ESA centered at 740 nm do not decay out to 200 ps, which is the maximum measured delay time. No clear blue-shifts are identified in this data.

ARTICLE

	Toluene	DMF	MeCN
TD1-Cu	2.3 ± 0.3 ps, 13.2 ± 1.1 ps	2.4 ± 0.4 ps, 7.8 ± 1.2 ps	1.7 ± 0.2 ps, 8.0 ± 1.0 ps
TD1-Cu-Ox	1.5 ± 0.1 ps, 10.7 ± 0.8 ps	2.0 ± 0.2 ps, 11.0 ± 0.5 ps	2.3 ± 0.2 ps, 11.5 ± 0.6 ps
TD1-Pd	0.8 ± 0.1 ps, 9.6 ± 1.1 ps	0.5 ± 0.1 ps, 7.4 ± 1.0 ps	0.6 ± 0.1 ps, 11.4 ± 1.8 ps
TD1-Pd-Ox	1.0 ± 0.1 ps, 60 ± 3.1 ps, 5*ns	0.4 ± 0.1 ps, 8 ± 1.0 ps, 6*ns	0.4 ± 0.1 ps, 40 ± 2.0 ps, 3*ns

Table 1: Lifetimes recovered from the global analysis performed on time-evolving transient spectra of TD1-Cu, TD1-Cu-Ox, TD1-Pd, and TD1-Pd-Ox reported with error bars generated from the standard error. *ns timescale outside of maximum time delay of experiment.

For the copper complexes, the timescales obtained for the neutral radical and the oxidized species are similar in all solvents. The timescales for the neutral radical palladium complex are faster but comparable to those found for the neutral radical copper molecules. The oxidized form of the palladium complex is an outlier. In all other molecules studied here, the transient absorption signal disappears, and the molecule returns to the ground state in tens of picoseconds. For TD1-Pd-Ox, there is a fast decay of the higher energy ESA and some relaxation of the bleach in tens of picoseconds, however, the excited state lifetime is significantly longer than the maximum time delay of the measurement (200 ps).

For the transient absorption data, the samples were excited in resonance with the lowest energy transition with significant oscillator strength, which is mainly localized on the ligand. The overall ligand dominance of the state is supported by experimental and computational observations. Comparison of the electrochemistry of the metal complexes indicates that the redox processes are occurring on the electron-rich conjugated π system of the ligand, with metal centers remaining in the same oxidation states.^{15, 16} Metal coordination red-shifts and changes the spectral shape but the lack of solvent polarity dependence indicates a weak ligand–metal charge-transfer character. Previously published results^{15, 16} indicate that while the metal center does have some involvement, the transitions primarily originate from the π system. EPR data further shows that the unpaired electron in the metal-bound neutral radical is delocalized over and accommodated by the ligand π system.¹⁶

The π to π^* nature of the primary transition in the visible means that redox or photophysical processes are relatively decoupled from the metal center. This potentially expands the types of processes that can be accommodated in a TD1-metal system, with those directly involving the metal center separated from the ligand. Although we do not observe it in our data, this could also involve chemical access to the metal center through the aqua ligand. In metalloporphyrins, the metal may

participate in the dynamics by dissociating an axial ligand. For the TD1 complexes, the coordinated aqua ligand is also hydrogen-bound to the tripyrindione ligand and its unfavorable dissociation would be readily apparent from changes in the absorption spectra following the measurement. Since we do not observe these spectral changes and the complex is stable during the experiment, we can conclude that the water ligand is retained.

Although the main transitions with large oscillator strength have π to π^* character, the metal center likely contributes to the fast non-radiative relaxation observed in the transient absorption data for all complexes. Non-radiative relaxation via coupling of the π to π^* transitions to a lower-lying metal states has been observed in many transition metal complexes. This deactivation pathway can result in significant non-radiative relaxation and has been a challenge in the development of photoluminescent complexes.^{45–47} In addition, the metalloporphyrin literature provides a wealth of precedents for such excited state deactivations caused by coupling with or mixing of the metal d-orbitals.^{29, 34, 40, 41, 43, 48–53} These states may be optically dark and have low oscillator strengths. However, energetic proximity and coupling of the metal to the dipole-allowed states can allow them to play a role in the relaxation of the excited state. The participation of a low-lying metal-centered state in the nonradiative relaxation of the excited state, is further supported by steady-state measurements on the d¹⁰ TD1-Zn complex, which has strong fluorescence in polar solvents.⁴⁴

The similarities between the transient absorption data for TD1-Cu, TD1-Cu-Ox, and TD1-Pd as well as the different dynamics observed for TD1-Pd-Ox can be explored by considering the electronic states. As has been shown in previous work, in all the complexes studied here, the metal center is in a square planar geometry^{16, 17}. In addition, the one-electron-oxidation of the complexes removes the electron from the ligand and not the metal center¹⁵. This means that the

palladium complexes have a diamagnetic d^8 Pd(II) center while the copper complexes have a paramagnetic d^9 open-shell Cu(II) center with an unpaired electron. Both neutral radical complexes have an electron occupying the conjugated π orbitals on the ligand. For TD1-Pd, this means that the ground state is a doublet with a singly occupied molecular orbital (SOMO) primarily localized on the ligand. For the copper neutral radical complex, TD1-Cu, the picture is a bit more complicated. The unpaired electron on the d^9 Cu(II) center is in the $d_{x^2-y^2}$ orbital and is nearly orthogonal to the electron localized on the ligand¹⁵. The ferromagnetic interaction between these unpaired electrons results in a triplet ground state. This situation is not unique to TD1-Cu and has been observed for other Cu(II) metal centers coordinated with planar radical ligands.⁵⁴⁻⁶⁰

In the one-electron-oxidized complexes, the electron on the ligand is removed and the oxidation state of the metal center remains the same. For TD1-Cu-Ox, the unpaired electron on the copper results in a doublet ground state. The oxidized palladium complex, TD1-Pd-Ox, is a closed shell system with a square planar d^8 Pd(II) metal center and the unpaired electron removed from the ligand. Of all the complexes studied here, TD1-Pd-Ox is the only one with a singlet state and for which we observe a long excited-state lifetime. The tunability enabled by a delocalized electron on the ligand and the ability of TD1 to bind multiple metals provides a method to select the overall spin state of the complex and to adjust the dynamics of the system.

For both the palladium and copper complexes, multiplet states may assist their non-radiative relaxation. For the neutral radical TD1-Pd, it is possible that as a heavy metal, palladium could promote intersystem crossing. For the copper complexes, if the orthogonality between the $d_{x^2-y^2}$ orbital and the π orbital on the ligand is not complete, the unpaired electron on the d^9 Cu(II) metal center can interact with the π system altering π singlet and triplet multiplicity through an exchange interaction^{33, 34, 37, 61, 62}. This would lead to fast intersystem crossing that could allow relaxation through an excited state of different multiplicity.

As shown in Fig. 3 (and in Fig. S1 and S2 in the ESI), the transient absorption spectra for both neutral radical complexes and the oxidized copper complex undergoes spectral evolution. For these complexes, the lower energy ESA features shift to higher energy. The TD1-Pd signals have a significant 60 nm blue-shift of the 690 nm ESA feature. Both TD1-Cu and TD1-Cu-Ox have relatively small, 15 nm and 20 nm, blue shifts of the ESA centered at approximately 645 nm and 740 nm, respectively. No blue shifts are observed for TD1-Pd-Ox. The spectral shift of an ESA to higher energies is likely associated with vibrational relaxation on the excited state⁶³⁻⁶⁷ as well as the loss of stimulated emission. This loss of stimulated emission could arise from transitions to a different multiplet state or through coupling to a lower-lying metal-centered state. These deactivation pathways would lead to rapid non-radiative relaxation of the excited state. In addition, the role of vibrational cooling and the loss of stimulated emission is supported by the narrowing of the ESA feature, which is

observed for all data except TD1-Pd-Ox. This narrowing is most apparent in the TD1-Pd data (Fig. 3 (d), (e)).

For all samples except the oxidized palladium complex, the timescales recovered from the data represent vibrational cooling followed by rapid non-radiative relaxation through a lower-lying state. This lower-lying state is likely metal-centered and may have a different multiplicity relative to the initially prepared excited state. Rapid non-radiative pathways are not favored for the oxidized palladium complex. This system consists of a Pd(II) cation coordinated to a closed-shell ligand with singlet ground and initially excited states. In Pd(II) porphyrin, which also consists of a Pd(II) cation complexed to a closed-shell ligand, the lifetime of the singlet state is on the order of tens of ps³² and the triplet state has a minimum lifetime of hundreds of ps.⁶⁸ In analogy to Pd(II) porphyrin, the long-lived excited state of TD1-Pd-Ox may be a triplet state.

Conclusions

Steady-state and femtosecond ultrafast time-resolved measurements were performed on copper and palladium complexes of tripyrrindione in both neutral radical and one-electron-oxidized forms. The steady-state and time-resolved spectra were found to be relatively insensitive to the solvent environment. Recovery of the ground state was observed within 10-100 ps for the copper and palladium neutral radical complexes as well as the oxidized copper complex, while the excited state lifetime of the oxidized palladium complex was significantly longer. Selection of the metal center and oxidation state of the complex allows for tuning of the overall spin of the ground and excited states. The stable open-shell configurations and the reversible redox activity of these novel tripyrrolic systems have potential applications for exploring magnetism and conductivity properties in molecule-based materials.

Author Contributions

Byungmoon Cho: Writing - Original Draft, Investigation, Conceptualization, Validation, Data Curation. Alicia Swain: Investigation, Validation. Ritika Gautam: Resources. Elisa Tomat: Resources, Writing - Review & Editing, Funding acquisition. Vanessa Huxter: Conceptualization, Methodology, Formal analysis, Software, Resources, Data Curation, Writing - Original Draft, Writing - Review & Editing, Visualization, Supervision, Project administration, Funding acquisition

Conflicts of interest

The authors declare no competing interests.

Acknowledgements

The authors gratefully acknowledge financial support from the UAREN program and the National Science Foundation (CAREER grant 1454047 to ET). VH thanks Prof. Scott Saavedra and Prof. Marek Romanowski for providing facility time and support.

Thanks to Clayton Curtis for helpful discussions. Funding for the facility was provided in part by NSF Major Research Instrumentation Grant 0958790.

References

1. L. Milgrom, *The Colours of Life: An Introduction to the Chemistry of Porphyrins and Related Compounds*, Oxford University Press, Oxford, 1997.
2. T. Mizutani and S. Yagi, *Journal of Porphyrins and Phthalocyanines*, 2004, **8**, 226-237.
3. A. B. Doust, K. E. Wilk, P. M. Curmi and G. D. Scholes, *Journal of Photochemistry and Photobiology A*, 2006, **184**, 1-17.
4. G. H. Krause and E. Weis, *Annual Review of Plant Physiology and Plant Molecular Biology*, 1991, **42**, 313-349.
5. R. J. Cogdell, T. D. Howard, N. W. Isaacs, K. McLuskey and A. T. Gardiner, *Photosynthesis Research*, 2002, **74**, 135-141.
6. D. X. Hu, D. M. Withall, G. L. Challis and R. J. Thomson, *Chemical Reviews*, 2016, **116**, 7818-7853.
7. R. Perez-Tomas and M. Vinas, *Current Medicinal Chemistry*, 2010, **17**, 2222-2231.
8. H. Falk, *The Chemistry of Linear Oligopyrroles and Bile Pigments*, Springer-Verlag Wien, 1 edn., 1989.
9. J. Beruter, J.-P. Colombo and U. P. Schlunegger, *European Journal of Biochemistry*, 1975, **56**, 239-244.
10. M. Bröring, in *Handbook of Porphyrin Science with Applications to Chemistry, Physics, Materials Science, Engineering, Biology and Medicine, Vol 8: Open-Chain Oligopyrrole Systems*, eds. K. M. Kadish, K. M. Smith and R. Guilard, World Scientific, Singapore, 2010, vol. 8, pp. 343-501.
11. E. Tomat, *Comments on Inorganic Chemistry*, 2016, **36**, 327-342.
12. S. K. Dey, S. Datta and D. A. Lightner, *Monatshefte für Chemie*, 2009, **140**, 1171-1181.
13. S. D. Roth, T. Shkindel and D. A. Lightner, *Tetrahedron*, 2007, **63**, 11030-11039.
14. E. Tomat and C. J. Curtis, *Accounts of Chemical Research*, 2021, **54**, 4584-4594.
15. R. Gautam, A. V. Astashkin, T. M. Chang, J. Shearer and E. Tomat, *Inorganic Chemistry*, 2017, **56**, 6755-6762.
16. R. Gautam, J. J. Loughrey, A. V. Astashkin, J. Shearer and E. Tomat, *Angewandte Chemie International Edition*, 2015, **54**, 14894-14897.
17. S. Bahn Müller, J. Plotzitzka, D. Baabe, B. Cordes, D. Menzel, K. Scharz, P. Schweyen, R. Wicht and M. Bröring, *European Journal of Inorganic Chemistry*, 2016, **2016**, 4761-4768.
18. M. Bröring, S. Prikhodovski and E. C. Tejero, *Chemical Communications*, 2007, **13**, 876-877.
19. M. Bröring and C. D. Brandt, *Chemical Communications*, 2001, **5**, 499-500.
20. M. Bröring and S. Prikhodovski, *Zeitschrift Für Anorganische Und Allgemeine Chemie*, 2008, **634**, 2451-2458.
21. M. Bröring, *Journal of Porphyrins and Phthalocyanines*, 2008, **12**, 1242-1249.
22. L. J. G. W. van Wilderen, C. N. Lincoln and J. J. van Thor, *Plos One*, 2011, **6**.
23. A. Swain, B. Cho, R. Gautam, C. J. Curtis, E. Tomat and V. Huxter, *The Journal of Physical Chemistry B*, 2019, **123**, 5524-5535.
24. M. Bröring, S. Prikhodovski, C. D. Brandt, E. C. Tejero and S. Kohler, *Dalton Trans.*, 2007, **2**, 200-208.
25. X. Wang, F. Q. Bai, M. Xie, L. Hao and H. X. Zhang, *Synth. Met.*, 2015, **210**, 258-267.
26. B. Liu, W. L. Yu, J. Pei, S. Y. Liu, Y. H. Lai and W. Huang, *Macromolecules*, 2001, **34**, 7932-7940.
27. M. Zhang, P. Lu, Y. G. Ma and J. C. Shen, *Journal of Physical Chemistry B*, 2003, **107**, 6535-6538.
28. T. Yasuda, I. Yamaguchi and T. Yamamoto, *Adv. Mater.*, 2003, **15**, 293-296.
29. M. Gouterman, *Journal of Molecular Spectroscopy*, 1961, **6**, 138-163.
30. M. Gouterman, in *The Porphyrins*, ed. D. Dolphin, Academic Press, New York, 1978, ch. 1, pp. 1-165.
31. A. Rosa and G. Ricciardi, in *Handbook of Porphyrin Science with Applications to Chemistry, Physics, Materials Science, Engineering, Biology and Medicine, Vol 22: Biophysical and Physicochemical Studies of Tetrapyrroles*, eds. K. M. Kadish, K. M. Smith and R. Guilard, 2012, vol. 22, pp. 169-234.
32. T. Kobayashi, K. D. Straub and P. M. Rentzepis, *Photochem. Photobiol.*, 1979, **29**, 925-931.
33. K. D. Straub, P. M. Rentzepis and D. Huppert, *Journal of Photochemistry*, 1981, **17**, 419-425.
34. D. Kim, D. Holten and M. Gouterman, *J. Am. Chem. Soc.*, 1984, **106**, 2793-2798.
35. A. Harriman, *Faraday Transactions*, 1981, **77**, 1281-1291.
36. G. V. N. Rajapakse, A. V. Soldatova and M. A. J. Rodgers, *Journal of Physical Chemistry B*, 2010, **114**, 14205-14213.
37. R. L. Ake and M. Gouterman, *Theoretica Chimica Acta*, 1969, **15**, 20-42.
38. A. Antipas, D. Dolphin, M. Gouterman and E. C. Johnson, *J. Am. Chem. Soc.*, 1978, **100**, 7705-7709.
39. D. Magde, M. W. Windsor, D. Holten and M. Gouterman, *Chemical Physics Letters*, 1974, **29**, 183-188.
40. J. B. Allison and R. S. Becker, *Journal of Chemical Physics*, 1960, **32**, 1410-1417.
41. J. B. Allison and R. S. Becker, *Journal of Physical Chemistry*, 1963, **67**, 2675-2679.
42. A. Harriman, *Journal of the Chemical Society-Faraday Transactions I*, 1981, **77**, 369-377.
43. M. D. Edington, W. M. Diffey, W. J. Doria, R. E. Riter and W. F. Beck, *Chemical Physics Letters*, 1997, **275**, 119-126.
44. R. Gautam, S. J. Petritis, A. V. Astashkin and E. Tomat, *Inorganic Chemistry*, 2018, **57**, 15240-15246.
45. O. S. Wenger, *Nature Chemistry*, 2020, **12**, 323-324.
46. O. S. Wenger, *Chemistry – A European Journal*, 2019, **25**, 6043-6052.
47. C. Förster and K. Heinze, *Chemical Society Reviews*, 2020, **49**, 1057-1070.
48. A. Antipas, D. Dolphin, M. Gouterman and E. C. Johnson, *J. Am. Chem. Soc.*, 1978, **100**, 7705-7709.
49. D. H. Kim, D. Holten, M. Gouterman and J. W. Buchler, *J. Am. Chem. Soc.*, 1984, **106**, 4015-4017.
50. A. Harriman, *Journal of the Chemical Society-Faraday Transactions I*, 1981, **77**, 369-377.
51. A. Harriman, *Journal of the Chemical Society-Faraday Transactions I*, 1981, **77**, 1281-1291.
52. R. S. Becker and J. B. Allison, *Journal of Physical Chemistry*, 1963, **67**, 2662-2669.

ARTICLE

Journal Name

53. R. S. Becker and J. B. Allison, *Journal of Physical Chemistry*, 1963, **67**, 2669-2675.
54. B. S. Erler, W. F. Scholz, Y. J. Lee, W. R. Scheidt and C. A. Reed, *J. Am. Chem. Soc.*, 1987, **109**, 2644-2652.
55. P. Chaudhuri, C. N. Verani, E. Bill, E. Bothe, T. Weyhermüller and K. Wieghardt, *J. Am. Chem. Soc.*, 2001, **123**, 2213-2223.
56. O. Kahn, R. Prins, J. Reedijk and J. S. Thompson, *Inorganic Chemistry*, 1987, **26**, 3557-3561.
57. C. Benelli, A. Dei, D. Gatteschi and L. Pardi, *Inorganic Chemistry*, 1990, **29**, 3409-3415.
58. A. Okazawa, D. Hashizume and T. Ishida, *J. Am. Chem. Soc.*, 2010, **132**, 11516-11524.
59. S. Ghorai, A. Sarmah, R. K. Roy, A. Tiwari and C. Mukherjee, *Inorganic Chemistry*, 2016, **55**, 1370-1380.
60. S. Konishi, M. Hoshino and M. Imamura, *J. Am. Chem. Soc.*, 1982, **104**, 2057-2059.
61. M. H. Ha-Thi, N. Shafizadeh, L. Poisson and B. Soep, *J. Phys. Chem. A*, 2013, **117**, 8111-8118.
62. M. Asano, Y. Kaizu and H. Kobayashi, *Journal of Chemical Physics*, 1988, **89**, 6567-6576.
63. M. M. Bishop, J. D. Roscioli, S. Ghosh, J. J. Mueller, N. C. Shepherd and W. F. Beck, *The Journal of Physical Chemistry B*, 2015, **119**, 6905-6915.
64. G. B. Shaw, C. D. Grant, H. Shirota, E. W. Castner, G. J. Meyer and L. X. Chen, *J. Am. Chem. Soc.*, 2007, **129**, 2147-2160.
65. O. Bilsel, S. N. Milam, G. S. Girolami, K. S. Suslick and D. Holten, *The Journal of Physical Chemistry*, 1993, **97**, 7216-7221.
66. D. Jeong, D.-G. Kang, T. Joo and S. K. Kim, *Scientific Reports*, 2017, **7**, 16865.
67. A. Marcelli, P. Foggi, L. Moroni, C. Gellini and P. R. Salvi, *The Journal of Physical Chemistry A*, 2008, **112**, 1864-1872.
68. D. Eastwood and M. Gouterman, *Journal of Molecular Spectroscopy*, 1970, **35**, 359-375.